Electronic Supplementary Information for the "The Jahn-Teller and pseudo-Jahn-Teller effects in propyne radical cation"

Arun Kumar Kanakati, Vadala Jhansi Rani and Susanta Mahapatra*

School of Chemistry, University of Hyderabad, Hyderabad 500 046, India

* Corresponding author, E-mail: susanta.mahapatra@uohyd.ac.in

STEPS TO ARRIVE AT EQS. 21-24

The diabatic quadratic $E\otimes e$-JT electronic Hamiltonian of the degenerate electronic state is given by

$$\Delta\mathcal{H} = \begin{bmatrix} u^x & u^{xy} \\ u^{xy} & u^y \end{bmatrix}, \tag{A1a}$$

with

$$u^{x/y} = E^0 + \sum_{i\epsilon a_1}\kappa_i Q_i + \frac{1}{2}\sum_{i\epsilon a_1}\gamma_i Q_i^2 \pm \sum_{i\epsilon e}\lambda_i Q_{ix} + \frac{1}{2}\sum_{i\epsilon e}\gamma_i(Q_{ix}^2 + Q_{iy}^2) \pm \frac{1}{2}\sum_{i\epsilon e}\eta_i(Q_{ix}^2 - Q_{iy}^2), \tag{A1b}$$

and

$$u^{xy} = \sum_{i\epsilon e}\left[\lambda_i Q_{iy} - 2\eta_i Q_{ix}Q_{iy}\right]. \tag{A1c}$$

Upon diagonalization of Eq. A1a, the adiabatic potential energy surfaces is obtained

$$\mathcal{V}_{\pm} = \frac{(u^x + u^y)}{2} \pm \left[\left(\frac{u^x - u^y}{2}\right)^2 + (u^{xy})^2\right]^{1/2}. \tag{A2a}$$

Substitution of Eqs. A1b and A1c into Eq. A2a and add addition of the harmonic potential of reference state $\mathcal{V}_0$ (Eq. 6 of the text) yields

$$\mathcal{V}_{\pm} + \mathcal{V}_0 = V_{\pm} = E^0 + \sum_{i\epsilon a_1}\kappa_i Q_i + \frac{1}{2}\sum_{i\epsilon a_1}\gamma_i Q_i^2 + \frac{1}{2}\sum_{i\epsilon a_1}\omega_i Q_i^2 + \frac{1}{2}\sum_{i\epsilon e}\gamma_i(Q_{ix}^2 + Q_{iy}^2) + \frac{1}{2}\sum_{i\epsilon e}\omega_i(Q_{ix}^2 + Q_{iy}^2)$$
$$\pm \left[\left(\sum_{i\epsilon e}\lambda_i Q_{ix} + \frac{1}{2}\sum_{i\epsilon e}\eta_i\left(Q_{ix}^2 - Q_{iy}^2\right)\right)^2 + \sum_{i\epsilon e}(\lambda_i Q_{iy} - 2\eta_i Q_{ix}Q_{iy})^2\right]^{1/2}. \tag{A2b}$$

The minimum of the seam of CIs occurs at the minimum of V_+ in the space of symmetric vibrational modes. Upon minimization of V_+ with respect to Q_i one obtains Eq. 23 (see text). Next the location of the minimum and saddle points of the lower adiabatic sheet are obtained by setting the first derivative of V_- with respect to the symmetric modes and degenerate modes to zero separately. Upon substitution of the results into V_- one obtains Eqs. 21 and 22 (see text). Note that absolute value of η_i distinguishes between minimum and saddle point. Finally the JT stabilization energy (Eq. 24) is obtained by subtracting Eq. 21 from Eq. 23.

TABLE S1. Higher order coupling parameters of $\widetilde{X}^2E$, $\widetilde{A}^2E$ states and PJT coupling between $\widetilde{A}^2E$-$\widetilde{B}^2A_1$ electronic states are derived from EOMIP-CCSD electronic structure data.

				$\widetilde{X}^2E$		
Mode	σ_i	σ_i'	δ_i	δ_i' (δ_i'')	ρ_i	ρ_i' (ρ_i'')
a_1						
ν_1	0.000898		0.001036			
ν_2	-0.000691		-			
ν_3	0.002899		-			
ν_4	-0.008080		-0.000832			
ν_5	-0.001012		-			
e						
ν_6	-0.0000007	0.0004	-	-	-	-
ν_7	-0.000013	0.0060	-	-	-	-
ν_8	-0.000011	0.0057	-	-	-	-
ν_9	0.00000009	0.0014	-0.00053	0.0000004 (0.0000006)	-0.00000003	-0.000953 (-0.001846)
ν_{10}	-0.000008	0.0078	0.00348	0.0000219 (0.0000286)	-	-

				$\widetilde{A}^2E$		
Mode	σ_i	σ_i'	δ_i	δ_i' (δ_i'')	ρ_i	ρ_i' (ρ_i'')
a_1						
ν_1	0.000670		0.000104			
ν_2	-		-			
ν_3	-		-			
ν_4	0.018160		0.008480			
ν_5	0.002170		-			
e						
ν_6	-0.00220	0.02060	0.00890	0.00011 (0.00011)	0.00150	-0.00360 (-0.00360)
ν_7	0.00008	0.00942	0.01822	-0.00001 (-0.00001)	-0.00005	-0.00397 (-0.00397)
ν_8	-0.00024	0.01210	0.00848	-0.00002 (-0.00002)	0.00019	-0.00335 (-0.00335)
ν_9	-0.00057	0.05901	-0.01472	0.00022 (0.00022)	0.00065	-0.00244 (-0.00244)
ν_{10}	-0.00001	0.00564	0.00129	0.00004 (0.00004)	-	-

		$\widetilde{A}^2E \times \widetilde{B}^2A_1$(PJT parameters)			
Mode	$\lambda_i'^{(3)}$	$\lambda_i'^{(4)}$	$\lambda_i'^{(4')}$	$\lambda_i'^{(5)}$	$\lambda_i'^{(5')}$
e					
ν_6	0.0528	-0.0070	-0.0070	-0.0067	-0.0067
ν_7	0.0767	-0.0108	-0.0108	-0.0094	-0.0094
ν_8	0.0161	-0.0031	-0.0031	-0.0019	-0.0019
ν_9	-0.0017	-0.0007	-0.0007	0.0007	0.0007
ν_{10}	0.0003	0.0001	0.0001	-	-

TABLE S2. Same as in Table S1 and the parameters are derived from CASSCF-MRCI electronic structure data.

Mode	σ_i	σ_i'	δ_i	$\delta_i'\ (\delta_i'')$	ρ_i	$\rho_i'\ (\rho_i'')$
			$\widetilde{X}^2E$			
a_1						
ν_1	0.000842		0.000785			
ν_2	-0.000850		-			
ν_3	0.002782		-			
ν_4	-0.008205		-0.001367			
ν_5	-0.001129		-			
e						
ν_6	-	-	-	-	-	-
ν_7	-0.000013	0.0060	-	-	-	-
ν_8	-0.000010	0.0059	-	-	-	-
ν_9	0.00000014	0.0025	0.000894	-0.000213 (0.000214)	-0.0000001	-0.000553 (-0.001538)
ν_{10}	-0.0000087	0.0071	0.000498	0.000010 (-0.000006)	-	-

Mode	σ_i	σ_i'	δ_i	$\delta_i'\ (\delta_i'')$	ρ_i	$\rho_i'\ (\rho_i'')$
			$\widetilde{A}^2E$			
a_1						
ν_1	0.0005796		-			
ν_2	-		-			
ν_3	-		-			
ν_4	0.0188956		0.0090729			
ν_5	0.0024462		-			
e						
ν_6	0.00073	-0.02796	0.02753	-0.000267 (-0.000267)	-0.00042	0.00310 (0.00310)
ν_7	-0.00002	0.02677	0.02656	0.000001 (0.000001)	0.00001	-0.00601 (-0.00601)
ν_8	-0.00030	0.02306	0.01037	-0.000020 (-0.000020)	0.00023	-0.00464 (-0.00464)
ν_9	-0.00048	0.04481	-0.03453	0.000263 (0.000263)	0.00051	0.00126 (0.00126)
ν_{10}	0.00039	0.00018	0.00406	0.000019 (0.000019)	-	-

Mode	$\lambda_i'^{(3)}$	$\lambda_i'^{(4)}$	$\lambda_i'^{(4')}$	$\lambda_i'^{(5)}$	$\lambda_i'^{(5')}$
			$\widetilde{A}^2E \times \widetilde{B}^2A_1$(PJT parameters)		
e					
ν_6	-0.0256	-0.0075	-0.0075	0.0080	0.0080
ν_7	0.0866	-0.0134	-0.0134	-0.0099	-0.0099
ν_8	0.0232	-0.0041	-0.0041	-0.0029	-0.0029
ν_9	-0.0094	-0.0010	-0.0010	0.0018	0.0018
ν_{10}	-0.0020	-0.0000	-0.0000	-	-

TABLE S3. The number of harmonic oscillator (HO) basis functions along the totally symmetric and degenerate vibrational modes and the dimension of the secular matrix used in the calculation of the stick vibrational spectra of the $\widetilde{X}^2E$, $\widetilde{A}^2E$ and $\widetilde{B}^2A_1$ electronic states of $CH_3CCH^{\cdot+}$ shown in various figures.

Electronic states	Vibrational modes	No. of HO basis	Dimension of secular matrix	Figure(s)
$\widetilde{X}^2E$	ν_1, ν_2, ν_3 ν_4, ν_5,	(10,12,20) (18,16)	691200	Figs. 5(b) and (c)
	ν_{6x}, ν_{6y}, ν_{7x}, ν_{7x} ν_{8x}, ν_{8y}, ν_{9x}, ν_{9y} ν_{10x}, ν_{10y}	(4,4,6,6) (8,8,4,4) (8,8)	37748736	Fig. 5(b) and (c)
$\widetilde{A}^2E$	ν_1, ν_2, ν_3 ν_4, ν_5,	(12,18,14) (20,16)	967680	Figs. 6(c) and (d)
	ν_{6x}, ν_{6y}, ν_{7x}, ν_{7x} ν_{8x}, ν_{8y}, ν_{9x}, ν_{9y}	(6,6,8,8) (8,8,4,4)	2359296	Fig. 6(e) and (f)
$\widetilde{B}^2A_1$	ν_1, ν_2, ν_3 ν_4, ν_5,	(14,12,16) (20,18)	967680	Figs. 5(c) and (d)

TABLE S4. Vibrational energy levels (in cm^{-1}) of the $\widetilde{X}^2E$, $\widetilde{A}^2E$ and $\widetilde{B}^2A_1$ electronic states of CH$_3$CCH$^{\cdot+}$ obtained from the uncoupled state calculations using the EOMIP-CCSD energy data. The assignment of the levels carried out by examining the nodal pattern of the wave functions is included in the table.

$\widetilde{X}^2E$				$\widetilde{A}^2E$			$\widetilde{B}^2A_1$	
Energy	Ref. [43]	Ref. [52]	Assignment	Energy	Ref. [43]	Assignment	Energy	Assignment
0			0_0^0	0		0_0^0	0	0_0^0
876	940	930±50	$\nu_{5_0}^1$	1024		$\nu_{5_0}^1$	917	$\nu_{5_0}^1$
1328			$\nu_{4_0}^1$	1304	1290	$\nu_{4_0}^1$	1497	$\nu_{4_0}^1$
1752			$\nu_{5_0}^2$	2048		$\nu_{5_0}^2$	1835	$\nu_{5_0}^2$
2169	1940	2000±50	$\nu_{3_0}^1$	2145		$\nu_{3_0}^1$	2018	$\nu_{3_0}^1$
2204			$\nu_{4_0}^1+\nu_{5_0}^1$	2328		$\nu_{4_0}^1+\nu_{5_0}^1$	2414	$\nu_{4_0}^1+\nu_{5_0}^1$
2628			$\nu_{5_0}^3$	2602		$\nu_{4_0}^2$	2752	$\nu_{5_0}^3$
2655			$\nu_{4_0}^2$	3073		$\nu_{5_0}^3$	2936	$\nu_{3_0}^1+\nu_{5_0}^1$
3046			$\nu_{3_0}^1+\nu_{5_0}^1$	3169		$\nu_{3_0}^1+\nu_{5_0}^1$	2991	$\nu_{4_0}^2$
3067			$\nu_{2_0}^1$	3178		$\nu_{2_0}^1$	3017	$\nu_{2_0}^1$
3080			$\nu_{4_0}^1+\nu_{5_0}^2$	3353		$\nu_{4_0}^1+\nu_{5_0}^2$	3332	$\nu_{4_0}^1+\nu_{5_0}^2$
3497			$\nu_{1_0}^1$	3449		$\nu_{3_0}^1+\nu_{4_0}^1$	3334	$\nu_{1_0}^1$
3498			$\nu_{3_0}^1+\nu_{4_0}^1$	3495		$\nu_{1_0}^1$	3515	$\nu_{3_0}^1+\nu_{4_0}^1$
3504			$\nu_{5_0}^4$	3626		$\nu_{4_0}^2+\nu_{5_0}^1$	3670	$\nu_{5_0}^4$
3531			$\nu_{4_0}^2+\nu_{5_0}^1$	3895		$\nu_{4_0}^3$	3853	$\nu_{3_0}^1+\nu_{5_0}^2$
3922			$\nu_{3_0}^1+\nu_{5_0}^2$	4097		$\nu_{5_0}^4$	3909	$\nu_{4_0}^2+\nu_{5_0}^1$
3943			$\nu_{2_0}^1+\nu_{5_0}^1$	4194		$\nu_{3_0}^1+\nu_{5_0}^2$	3935	$\nu_{2_0}^1+\nu_{5_0}^1$
3956			$\nu_{4_0}^1+\nu_{5_0}^3$	4202		$\nu_{2_0}^1+\nu_{5_0}^1$	4036	$\nu_{3_0}^2$
3980			$\nu_{4_0}^3$	4377		$\nu_{4_0}^1+\nu_{5_0}^3$	4252	$\nu_{1_0}^1+\nu_{5_0}^1$
4339			$\nu_{3_0}^2$	4482		$\nu_{2_0}^1+\nu_{4_0}^1$	5036	$\nu_{2_0}^1+\nu_{3_0}^1$
4373			$\nu_{1_0}^1+\nu_{5_0}^1$	4520		$\nu_{1_0}^1+\nu_{5_0}^1$	5352	$\nu_{1_0}^1+\nu_{3_0}^1$
4380			$\nu_{5_0}^5$	4651		$\nu_{4_0}^2+\nu_{5_0}^2$	6035	$\nu_{2_0}^2$
4395			$\nu_{2_0}^1+\nu_{4_0}^1$	4747		$\nu_{3_0}^1+\nu_{4_0}^2$		
4407			$\nu_{4_0}^2+\nu_{5_0}^2$	5218		$\nu_{3_0}^1+\nu_{5_0}^3$		
				5227		$\nu_{2_0}^1+\nu_{5_0}^2$		
				5323		$\nu_{2_0}^1+\nu_{3_0}^1$		
				5544		$\nu_{1_0}^1+\nu_{5_0}^2$		

TABLE S5. Same as in Table S4 obtained with the set of parameters derived from the CASSCF-MRCI energy data.

$\widetilde{X}^2E$				$\widetilde{A}^2E$			$\widetilde{B}^2A_1$	
Energy	Ref. [43]	Ref. [52]	Assignment	Energy	Ref. [43]	Assignment	Energy	Assignment
0			0_0^0	0		0_0^0	0	0_0^0
876	940	930±50	ν_{50}^1	1033		ν_{50}^1	914	ν_{50}^1
1341			ν_{40}^1	1315	1290	ν_{40}^1	1495	ν_{40}^1
1753			ν_{50}^2	2067		ν_{50}^2	1828	ν_{50}^2
2168	1940	2000±50	ν_{30}^1	2156		ν_{30}^1	1995	ν_{30}^1
2218			$\nu_{40}^1+\nu_{50}^1$	2348		$\nu_{40}^1+\nu_{50}^1$	2409	$\nu_{40}^1+\nu_{50}^1$
2630			ν_{50}^3	2622		ν_{40}^2	2742	ν_{50}^3
2680			ν_{40}^2	3100		ν_{50}^3	2909	$\nu_{30}^1+\nu_{50}^1$
3045			$\nu_{30}^1+\nu_{50}^1$	3183		ν_{20}^1	2988	ν_{40}^2
3067			ν_{20}^1	3189		$\nu_{30}^1+\nu_{50}^1$	3016	ν_{20}^1
3095			$\nu_{40}^1+\nu_{50}^2$	3382		$\nu_{40}^1+\nu_{50}^2$	3279	ν_{10}^1
3504			ν_{10}^1	3471		$\nu_{30}^1+\nu_{40}^1$	3323	$\nu_{40}^1+\nu_{50}^2$
3509			$\nu_{30}^1+\nu_{40}^1$	3499		ν_{10}^1	3491	$\nu_{30}^1+\nu_{40}^1$
3557			$\nu_{40}^2+\nu_{50}^1$	3656		$\nu_{40}^2+\nu_{50}^1$	3656	ν_{50}^4
3922			$\nu_{30}^1+\nu_{50}^2$	3922		ν_{40}^3	3823	$\nu_{30}^1+\nu_{50}^2$
3944			$\nu_{20}^1+\nu_{50}^1$	4133		ν_{50}^4	3902	$\nu_{40}^2+\nu_{50}^1$
3972			$\nu_{40}^1+\nu_{50}^3$	4216		$\nu_{20}^1+\nu_{50}^1$	3930	$\nu_{20}^1+\nu_{50}^1$
4017			ν_{40}^3	4223		$\nu_{30}^1+\nu_{50}^2$	3991	ν_{30}^2
4337			ν_{30}^2	4312		ν_{30}^2	4193	$\nu_{10}^1+\nu_{50}^1$
4381			$\nu_{10}^2+\nu_{50}^1$	4415		$\nu_{40}^1+\nu_{50}^3$		
4386			ν_{50}^5	4498		$\nu_{20}^1+\nu_{40}^1$		
4408			$\nu_{20}^1+\nu_{40}^1$	4532		$\nu_{10}^1+\nu_{50}^1$		
				4689		$\nu_{40}^2+\nu_{50}^2$		
				4779		$\nu_{30}^1+\nu_{40}^2$		
				5256		$\nu_{30}^1+\nu_{50}^3$		
				5339		$\nu_{20}^1+\nu_{30}^1$		
				5346		$\nu_{30}^2+\nu_{50}^1$		

TABLE S6. Normal mode combinations, sizes of the primitive and single particle bases used in the MCTDH calculations. [a] The primitive basis consists of harmonic oscillator DVR functions, in the dimensionless normal coordinate required to represent the system dynamics along the relevant mode. The primitive basis for each particle is the product of the one-dimensional bases; [b] The SPF basis is the number of the single particle functions used.

Electronic state	Normal modes	Primitive basis[a]	SPF basis[b]	
$\widetilde{X}^2E$	$\nu_1,\ \nu_{6x},\ \nu_{6y},\ \nu_2$	(6,10,10,8)	[8,8]	
	$\nu_4,\ \nu_{7x},\ \nu_{7y},\ \nu_3$	(16,14,14,14)	[8,8]	Fig. 7(b) and (c)
	$\nu_{8x},\ \nu_{8y},\ \nu_5$	(16,16,10)	[8,8]	
	$\nu_{9x},\nu_{9y},\nu_{10x},\nu_{10y}$	(12,12,16,16)	[10,10]	
$\widetilde{A}^2E\ \&\widetilde{B}^2A_1$	$\nu_1,\ \nu_{6x},\ \nu_{6y},\ \nu_2$	(10,12,12,14)	[22,22,12]	
	$\nu_4,\ \nu_{7x},\ \nu_{7y},\ \nu_3$	(12,18,18,18)	[24,24,12]	Fig. 7(b) and (c)
	$\nu_{8x},\ \nu_{8y},\ \nu_5$	(16,16,14)	[22,22,12]	
	$\nu_{9x},\ \nu_{9y},$	(12,12)	[20,20,10]	

(a)876 cm^{-1}

(b)1328 cm^{-1}

(c)2170 cm^{-1}

(d)1752 cm^{-1}

(e)2655 cm^{-1}

(f)4340 cm^{-1}

(g)2628 cm^{-1}

(h)3980 cm^{-1}

(i)2604 cm^{-1}

(j)3046 cm^{-1}

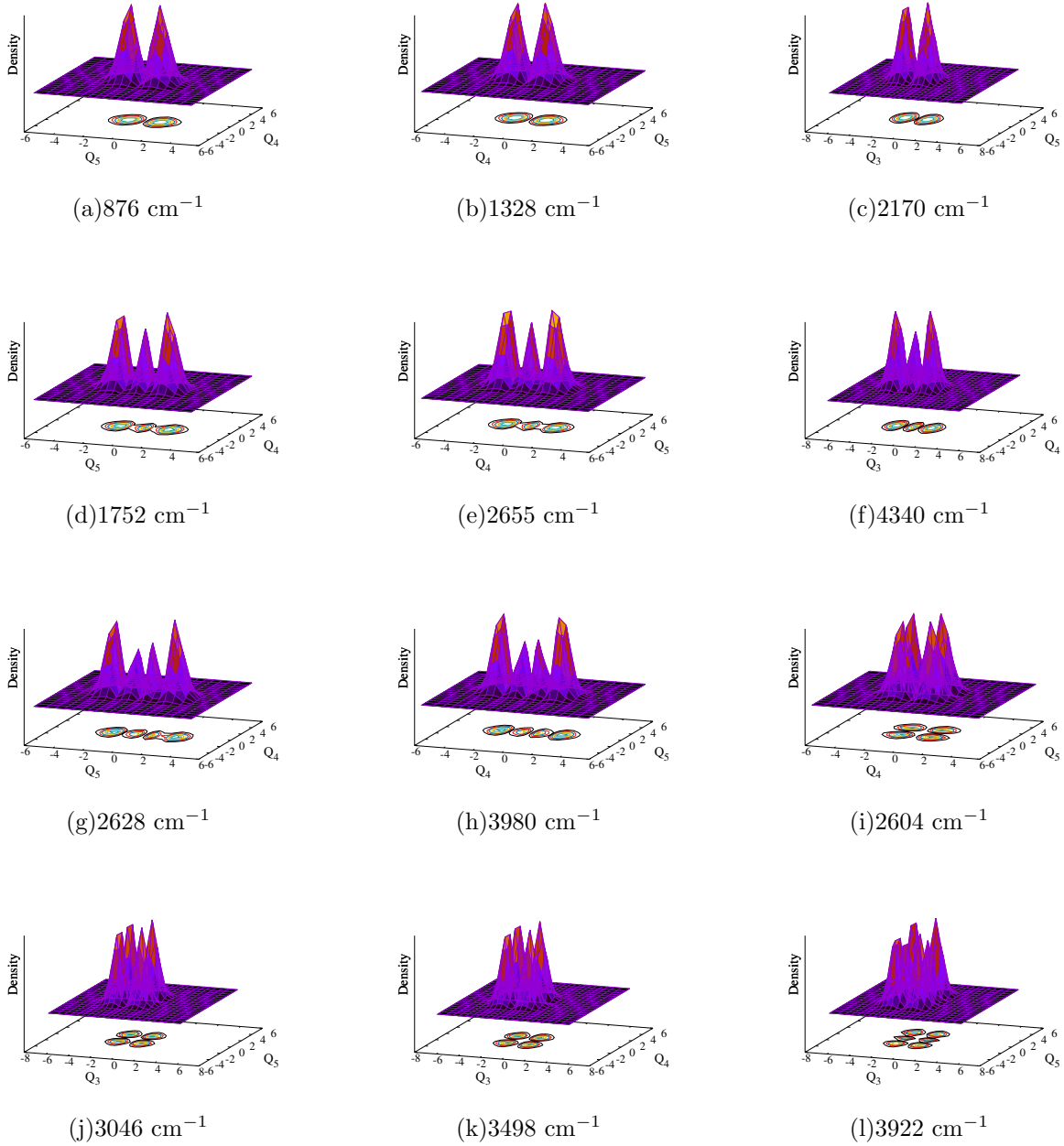(k)3498 cm^{-1}
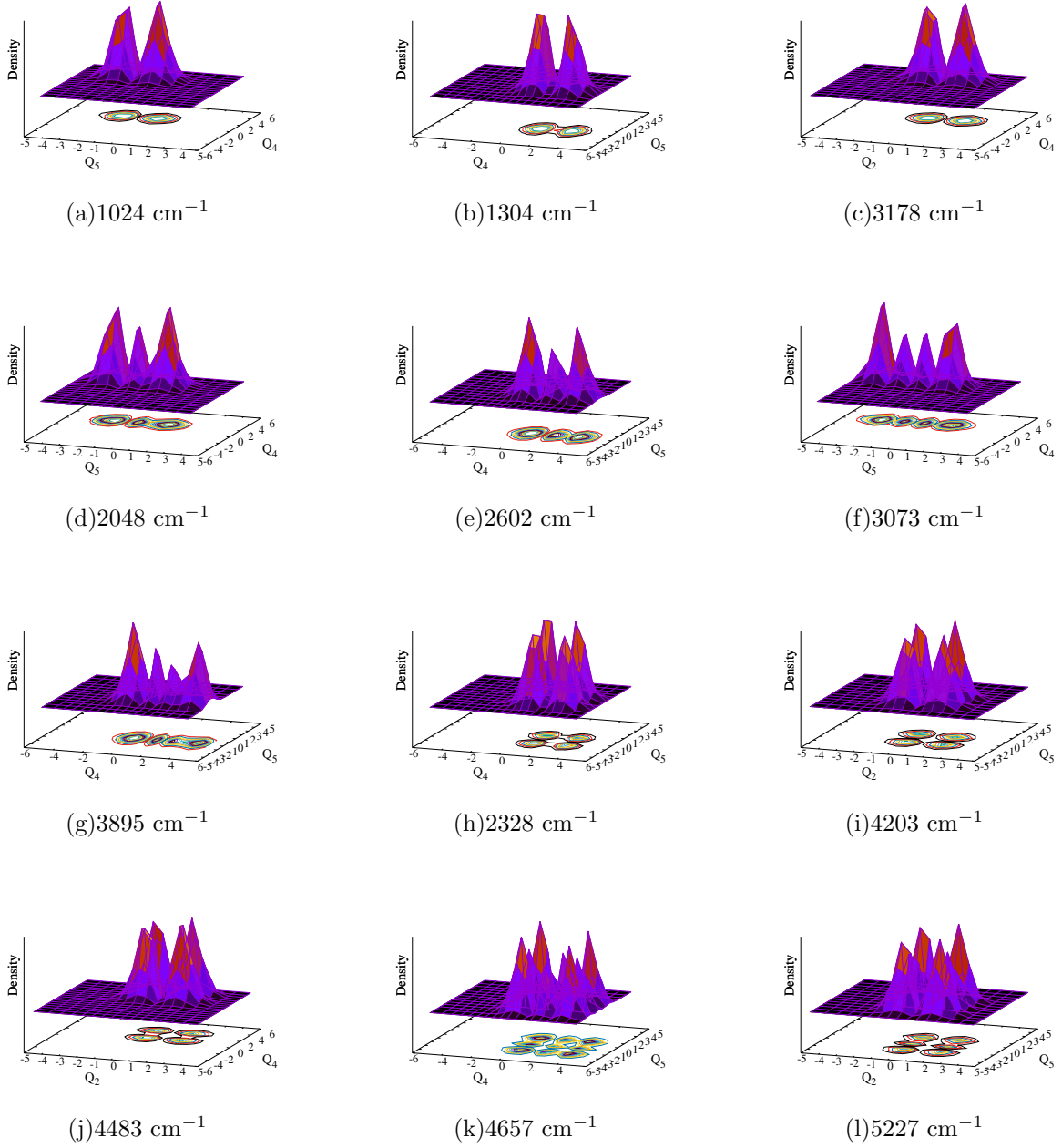
(l)3922 cm^{-1}

FIG. S1. Probability density of vibronic wave functions of the $\widetilde{X}^2E$ electronic state of $CH_3CCH^{\cdot+}$ as a function of nuclear coordinate. The EOMIP-CCSD Hamiltonian parameters are used in the calculations. Panels a-c and d-f represent the fundamentals and first overtone of ν_5, ν_4 and ν_3 vibrational modes, respectively. Panels g and h represent the second overtone of ν_5 and ν_4 modes. The wave functions in panels i-l represent the combination peaks of ν_5, ν_4 andν_3 modes.

9

(a)1024 cm^{-1} (b)1304 cm^{-1} (c)3178 cm^{-1}

(d)2048 cm^{-1} (e)2602 cm^{-1} (f)3073 cm^{-1}

(g)3895 cm^{-1} (h)2328 cm^{-1} (i)4203 cm^{-1}

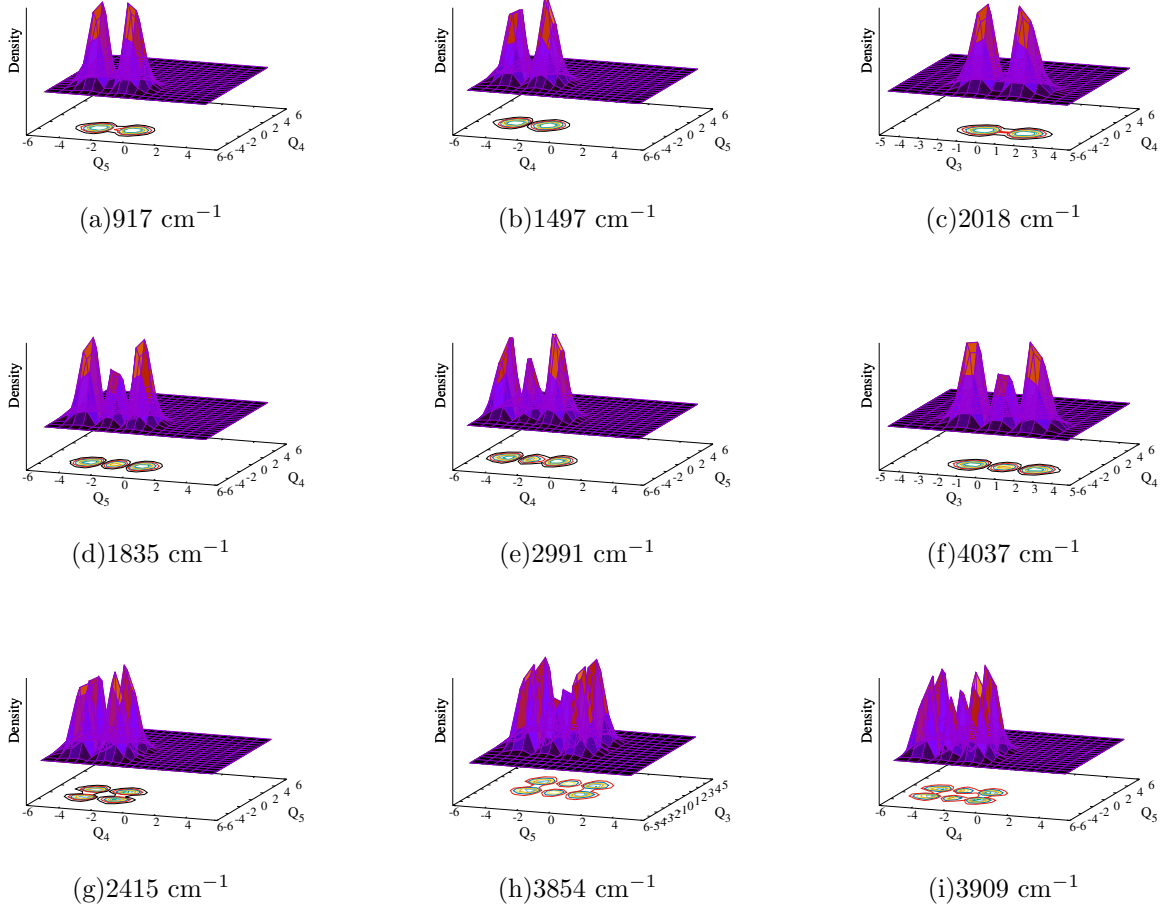(j)4483 cm^{-1} (k)4657 cm^{-1} (l)5227 cm^{-1}

FIG. S2. Probability density of vibronic wave functions of the $\widetilde{A}^2E$ electronic state of $CH_3CCH^{\cdot+}$ as a function of nuclear coordinate. The EOMIP-CCSD Hamiltonian parameters are used in the calculations. Panels a-c and d-e represent the fundamentals and first overtone of ν_5, ν_4 and ν_2 vibrational modes, respectively. Panels f and g represent the second overtone of ν_5 and ν_4 modes. The wave functions in panels h-l represent the combination peaks of ν_5, ν_4 and ν_2 modes.

FIG. S3. Probability density of vibronic wave functions of the $\widetilde{B}^2 A_1$ electronic state of $CH_3CCH^{\cdot+}$ as a function of nuclear coordinate. The EOMIP-CCSD Hamiltonian parameters are used in the calculations. Panels a-c and d-f represent the fundamentals and first overtone of ν_5, ν_4 and ν_3 vibrational modes, respectively. The wave functions in panels g-i represent the combination peaks of ν_5, ν_4 and ν_3 modes.